Bathymetry, Geomagnetic and Gravity Anomalies of the Mid-Atlantic Ridge between 14°N and 16°N

Toshiya FUJIWARA *1 Takeshi MATSUMOTO *1 Peter B. KELEMEN *2
Masato JOSHIMA *3 John F. CASEY *4 Akira TAKEUCHI *5
Georges M. CEULENEER *6 Michael G. BRAUN *2 Satoru KANDA *7

The Mid-Atlantic Ridge between 14°N and 16°N is supposed to be in a magma-starved portion of a slow spreading ridge, where igneous crust is virtually absent and rocks of the lower crust and upper mantle are distributed on the seafloor over about 100 km along the strike. The melting process, melt migration mechanisms, crustal deformation mechanisms during the magma-starved tectonic seafloor spreading: these are fundamental questions for the understanding of global mid-ocean ridge systems. A geophysical survey was conducted in June and July 1998 aboard the R/V Yokosuka to characterize geophysically the on and off-axis ridge flanks. The survey tracks covered a distance from 60 km north to 140 km south of the 15°20'N Fracture Zone. The tracks reached to 70 km off the ridge axis on both sides, the crustal age of which is about 5 m.y. old. Low amplitude geomagnetic anomalies and magnetization variation, compared with more magmatically robust parts of the Mid-Atlantic Ridge, were observed. This is consistent with the exposure of peridotite due to limited basaltic magma supply over a period of several million years. Low amplitude "bull's eye" mantle Bouguer anomalies were observed on the ridge segments flanking the active transform fault. This is probably due to a limited magma supply, thus this region has not generated thick igneous oceanic crust. The gravity data support the conclusion that the magma-starved nature of the region is a long lived phenomenon. Small amplitudal variations of mantle Bouguer anomalies across the ridge axis may suggest that the density structure or crustal thickness varies with time over about 2 m.y., thus the tectonic activity may be cyclic. The largest mantle Bouguer gravity anomalies are lows along the ridge axis at the northernmost and southernmost limits of our survey area. The simplest interpretation of these data seems to be that the large gravity lows represent the centers of unusually large magmatic segments at approximately 14°N and 16°N, probably as a result of 3-dimensional focusing of melt generation processes in the mantle.

Key words : Mid-Atlantic Ridge, 15°20'N Fracture Zone, Bathymetry, Gravity Anomaly,Geomagnetic Anomaly

* 1 Deep-Sea Research Department, Japan Marine Science and Technology Center
* 2 Department of Geology and Geophysics, Woods Hole Oceanographic Institution
* 3 Marine Geology Department, Geological Survey of Japan
* 4 Department of Geosciences, University of Houston
* 5 Department of Earth Sciences, Toyama University
* 6 CNRS OMP, Toulouse
* 7 Nippon Marine Enterprises, Co. Ltd.

1. Introduction

The Mid-Atlantic Ridge between 14°N and 16°N issupposed to be in a magma-starved portion of a slow spreading ridge, where igneous crust is virtually absent and rocks of the lower crust and upper mantle are distributed on the seafloor over about 100 km along the strike (e.g. Cannat et al., 1997). The melting process, melt migration mechanisms, crustal deformation mechanisms during the magma-starved tectonic seafloor spreading: these are fundamental questions for the understanding of global mid-ocean ridge systems. The YK98-05 Shinkai/ Yokosuka cruise (MODE '98 Leg 1) was conducted in this portion of the Mid-Atlantic Ridge from June 17th to July 17th 1998 (Sun Juan, Puerto Rico - Lisbon, Portugal). The aim of the dive survey aboard the research submersible Shinkai 6500 was to characterize upper mantle geochemistry. Particular emphasis was placed on determining the variation of these characteristics along the axis (Kelemen et al., 1998; Matsumoto et al., 1998). At nighttime and on the submersible's maintenance days, geophysical surveys, whose items included were swath bathymetry, geomagnetics and gravity, were conducted aboard the R/V Yokosuka. The aim of the geophysical surveys was to provide a geophysical characterization of the on and off-axis ridge flanks, which will be used to unravel tectonic evolution and crustal structure, both in the vicinity of the fracture zone and in the adjacent ridge segments (Fujiwara et al., 1999).

2. Data Acquisition and Processing

2.1 Swath Bathymetry

Survey tracklines were designed to orient all tracklines at least 10°, and up to about 25-30°, to plate flowlines to assure that real morphological features, which are normally oriented parallel and perpendicular to flowlines, can be distinguished from artifacts caused by beam-point errors in multibeam bathymetry (Fig. 1). Track spacing near the outer edge of the survey was about 6-7 km, and track spacing over the crest of the rift mountains again was about 5 km to get complete bathymetric coverage, excepting occasional shallow ridges. The survey tracks covered a distance from 60 km north to 140 km

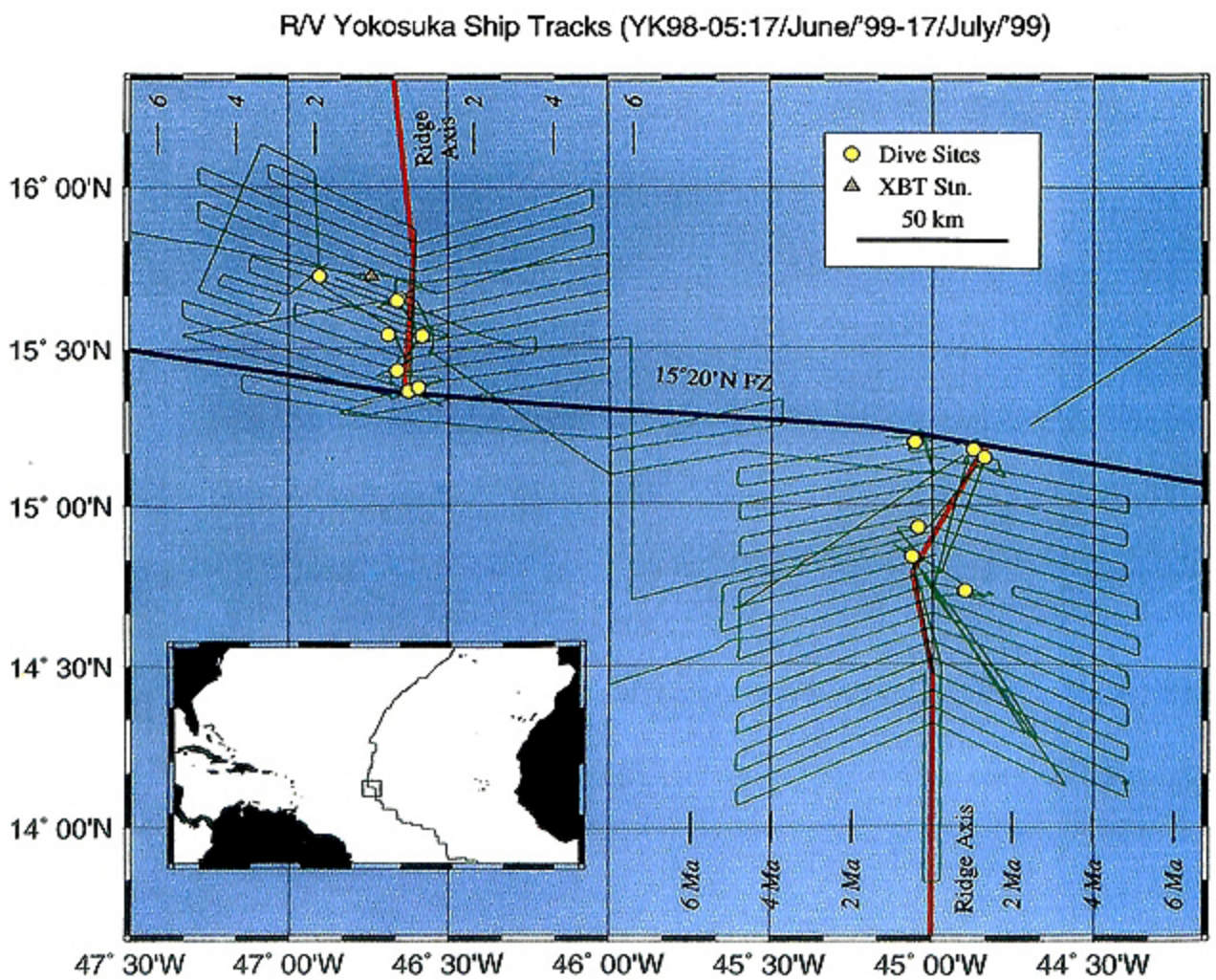

Fig. 1 Survey ship tracks of the YK98-05 cruise. Solid circles show the submersible Shinkai 6500 dive sites. A triangleshows an XBT station. Thick solid lines delineate ridge axes and the 15°20'N Transform Fault.

south of the 15°20'N Fracture Zone. The tracks reached to 70 km off the ridge axis on both sides, the crustal age of which is about 5 m.y. old (DeMets et al., 1990). In the study area, the total length of the geophysical measurement tracks amounted to about 3,700 nautical miles (7,000 km), and 27,000 km² areal coverage was obtained. Differential observation of Global Positioning System (D-GPS) and World Geodetic System (WGS) 84 geographical coordinates were used to provide the geographical position, and Greenwich Mean Time (GMT) was used for shipboard operations throughout this survey. Bathymetric data were collected using a HS-10 multi-narrow beam echo sounder surveying system. The HS-10 has 45 beams and a swath width of 90°, which covers a total of double the water depth. The sound velocity profile in the water column for depth calculation was based on the measurement of an expendable bathothermograph (XBT) at 15°43.5'N, 46°44.5'W (Fig. 1 and 2).

The bathymetric data were collected with data distribution density of 100-200 m space interval. The small number of artifacts included the occasional "curl-up" of the outermost beams and a few totally spurious depth readings. About 5 % of beam points were edited out. Positioning errors, from 22:00 on June 23 1998 to 0:00 on June 24 1998 GMT and from 10:00 on June 24 1998 to 22:50 on June 24 1998 GMT, were corrected. Cross over errors in center beam depth within the YK98-05 data set have a mean value of 3.5±31.0 m (Fig. 3). Errors between the common grid nodes of the YK98-05 and a bathymetry dataset of a previous cruise obtained by a French research group have a mean value of 2.7±31.8 m in the northern study area, and of 3.9±28.0 m in the southern area (Fig. 4). The two datasets were merged after the correction by adding these mean depth offsets of 2.7 m in the northern area and 3.9 m in the southern area, respectively. Data were gridded at 0.1' by 0.1' (179 m in longitude by 185 m in latitude) cell size in order to even out the data density while preserving the characteristic high resolution of multibeam data.

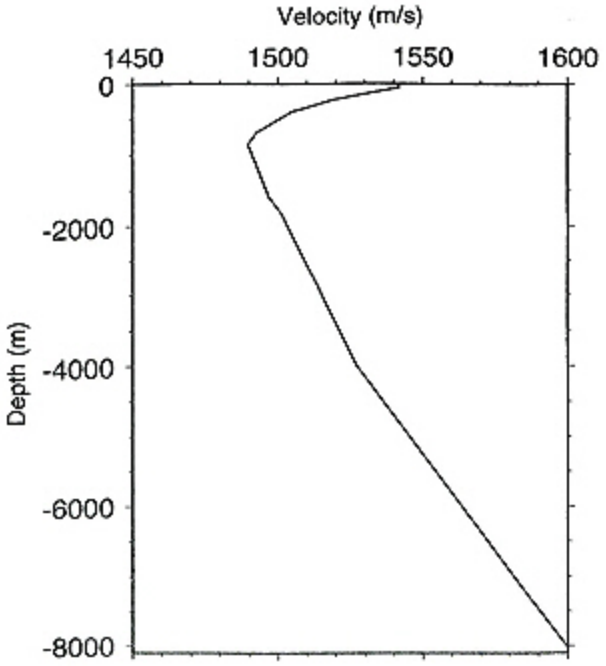

Fig. 2 Sound velocity profile in the study area.

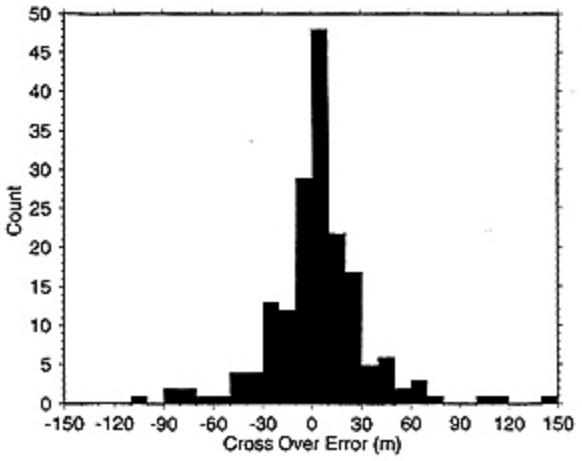

Fig. 3 Histogram of cross over errors of the center beam bathymetry in the YK98-05 survey.

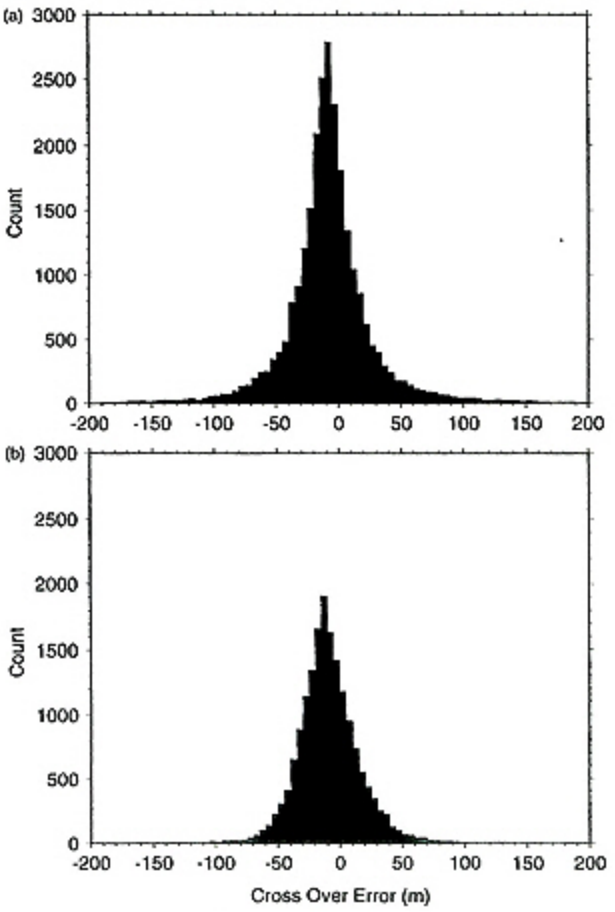

Fig. 4 Histogram of differences between the YK98-05 and the French surveys. (a) north of the 15°20'N Fracture Zone. (b) south of the 15°20'N Fracture Zone.

2.2 Geomagetics

Geomagnetic total force data were obtained by using a surface-towed proton precession magnetometer STC10 (Kawasaki Geol. Eng. Co.). The sensor was towed 350 m behind the ship. The data were collected every 20 seconds. After positioning correction taking into account the sensor cable length, the geomagnetic total force anomaly was calculated by subtracting the International Geomagnetic Reference Field (IGRF) 1995 model (IAGA, 1995) as the reference field and by offsetting the DC field of -60 nT from the observed field. The data yielded cross over errors of 3.4±22.3 nT. Diurnal variation was estimated by using the geomagnetic field observations themselves and reduced. The method uses the anomalies and differences at track crossovers to produce an acceptable diurnal variation curve (Buchanan et al., 1996). Corrected anomalies reduce cross over errors of up to -2.7±13.5 nT (Fig. 5).

Vector magnetic field data were collected using a shipboard three-component magnetometer, Tierra Tecnica SFG-1212, with a Tokimec ES-110 gyrocompass and a vertical reference unit of the HS-10 multi-narrow beam echo sounder. The data sampling rate was 8 Hz. The vector geomagnetic field was derived from the observed magnetic field using the formulation described in Appendix (Isezaki, 1986). "Figure-8 turn"s (a ship runs along an 8-shaped track consisting of two circles) were made three times for calibration of the ship's magnetic effect (Table 1). The vector geomagnetic anomaly was also calculated by subtracting the IGRF 1995 model from the observed field. The resultant anomalies suffered from strong bias. DC fields were removed from the observed field with each track unit.

Table 1 Log of "Figure-8 turn"s.

St.	Date(GMT)	Location
1	20/6/98 18:10-18:22	15° 43.7'N, 46° 46.2'W
2	01/7/98 21:43-21:55	14° 55.8'N, 45° 00.2'W
3	08/7/98 17:57-18:25	14° 08.5'N, 44° 23.9'W

Table 2 On-land gravity measurements.

St.	Date(Local Time)	G-1039 Gravity	Absolute Gravity	S-63 Gravity	Location
1	19/5/98 15:20	3340.90	979758.1	10871.4	JAMSTEC
2	16/6/98 09:16	2247.54	978664.5		Pier-3, Sun Juan, Puerto Rico
3	16/6/98 09:41	2249.75	978666.7		Frontier Base Pier, Sun Juan
4	16/6/98 11:24	2245.06	978662.0		Capital Dome, Sun Juan
5	16/6/98 12:17	2247.55	978664.5	9779.4	Pier-3, Sun Juan
6	17/7/98 14:54	3655.29		11201.0	Pier St. Apolonia, Lisbon, Portugal
7	17/7/98 16:20	3655.13	980079.8		Pier St. Apolonia, Lisbon
8	17/7/98 18:06	3665.39	980089.3		Doca Da Alcantara, Lisbon
9	17/7/98 18:25	3663.10	980087.9		Eastern End of Doca Da Alcantara, Lisbon
10	17/7/98 18:56	3655.34		11200.9	Pier St. Apolonia, Lisbon

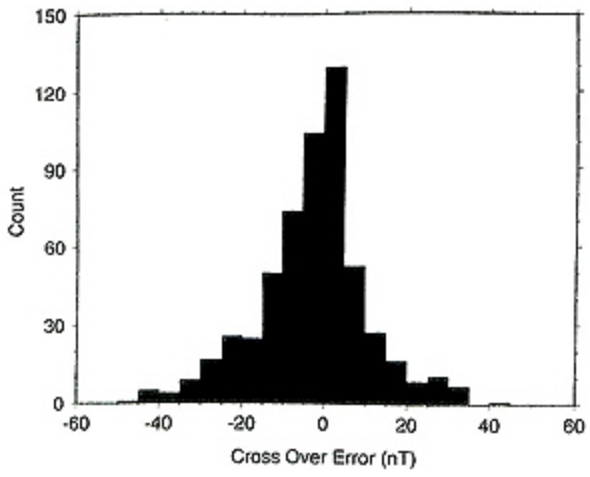

Fig. 5 Histogram of cross over errors of the geomagnetic total intensity anomalies.

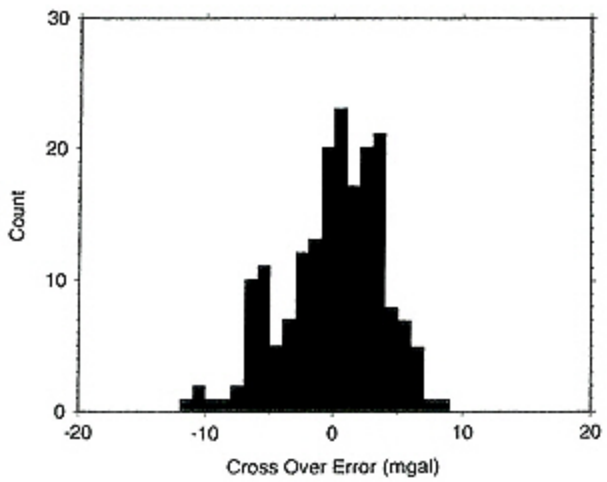

Fig. 6 Histogram of cross over errors of the free-air gravity anomalies.

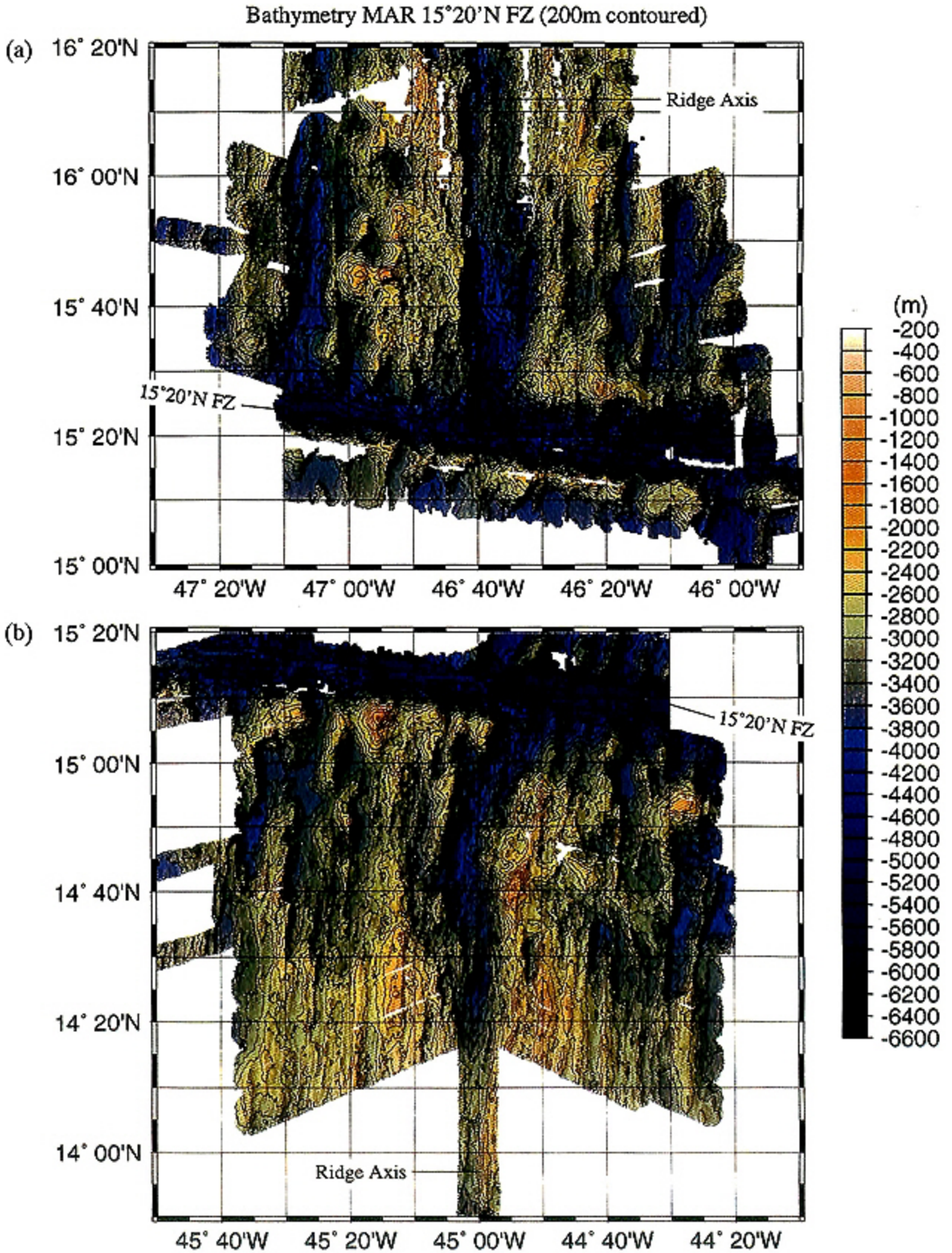

Fig. 7 Bathymetric map of the Mid-Atlantic Ridge. Contours are at 100 m intervals. (a) north of the 15°20'N Fracture Zone. (b) south of the 15°20'N Fracture Zone.

2.3 Gravity

Gravity data along the ship tracks were collected using the LaCoste & Romberg shipboard gravimeter S-63. The data were recorded every 10 seconds. Shipboard gravity data were tied to absolute gravity values at some reference points measured using LaCoste & Romberg gravimeter G-1093 (Table 2). After Eötvös correction and sensor drift correction with the rate of 0.12 mgal/day, free-air gravity anomaly was calculated by subtracting the theoretical gravity formula of the Geodetic Reference System 1967 from the observed data. A total of 203 track crossings for estimation of crossover errors were obtained during this cruise. Crossover errors have a mean value of -0.5 mgal and a standard deviation of 3.4 mgal (Fig. 6).

3. Summary of Observational Results

3.1 Swath Bathymetry

The median valley of the ridge axis in the north of the 15°20'N Fracture Zone trends in the N-S direction (Figure 7(a)). Morphological trend of about N10°E is found on the ridge flanks and in the median valley as well as the N-S trending. The direction of N10°E corresponds to the normal direction of the flowline of plate spreading estimated by a global analysis (DeMets et al., 1990). Along axis discontinuity, represented by a transition from dome shaped highlands to rift mountains, is traced in the western flank from the ridge axis at 15°50'N in the strike of N60°W. The ridge flanks from the fracture zone to 15°50'N show asymmetrical morphology (Figures 7(a) and 8(a)). Dome-shaped topographic highs are dominant in the western flank. Flowline-parallel corrugations (mullion structure) associated with long-lived faults at some places were found (Casey et al., 1998). A dome-shaped topographic high located 30 km west of the northern segment, termed a "megamullion" was identified. Gabbro and peridotite were collected by the Shinkai 6500 along a transect up the southern slope of this feature and upper mantle rocks on the seafloor on very long-lived, low angle faults due to tectonic seafloor spreading in the absence of magmatism. In contrast, topographic depressions deeper than 3,000 m are dominant except inside corner highs in the eastern flank.

The 15°20'N Fracture Zone is lineated in a direction of about N100°E. From 46°40'W to 45°55'W, the fracture zone (transform fault) has another lineation in a direction of about N90°E. The ridge axis is running in the strike of about N10°E between the eastern ridge-transform intersection and 14°40'N (Figure 7(b)). In these off-ridge flanks, two topographic lineations of N10°E and N-S coexist. The ridge flanks show asymmetry: the western flank is shallower than the eastern flank except inside corner highs (Figures 7(b) and 8(b)). Seamount-like topographic

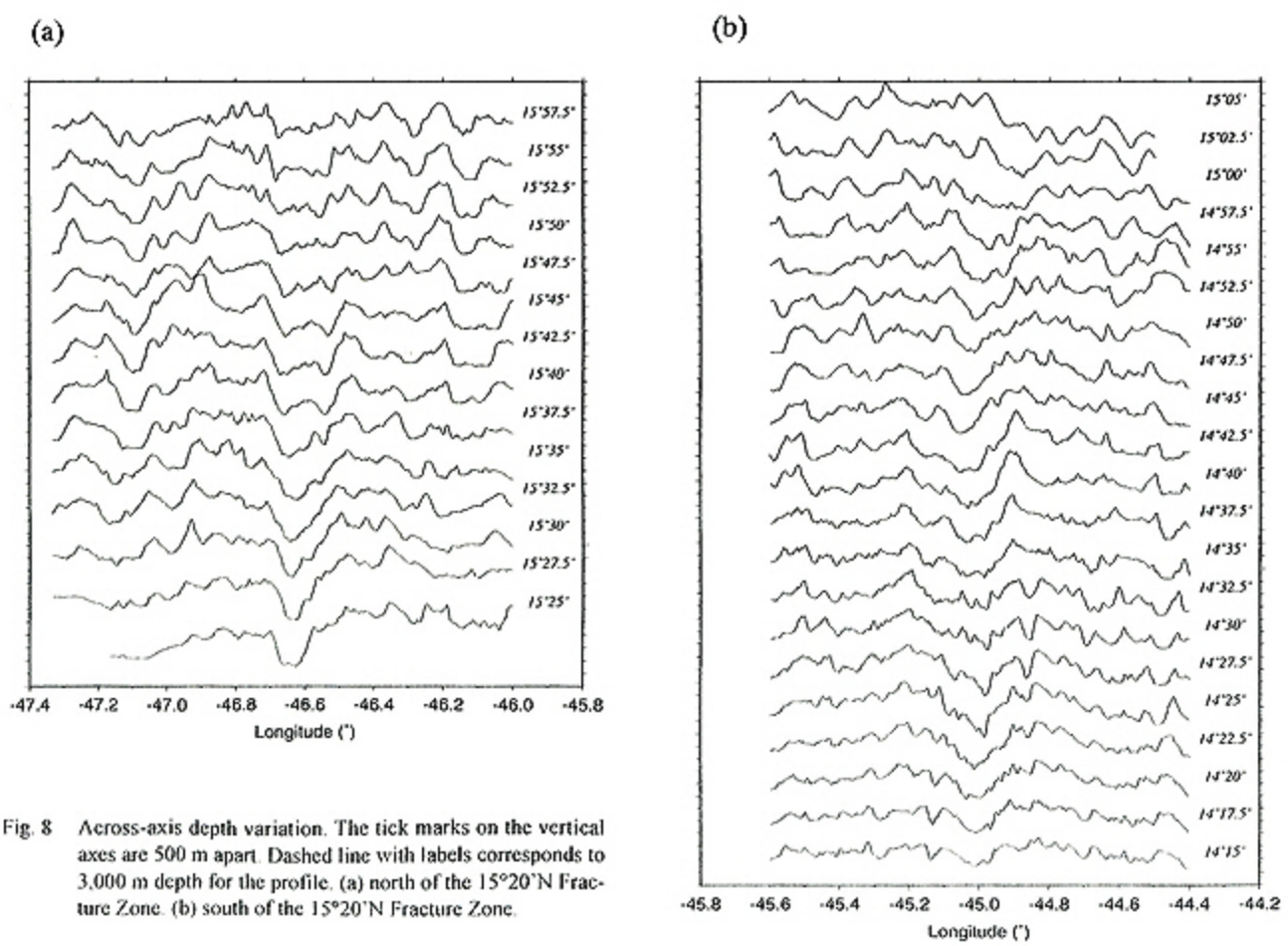

Fig. 8 Across-axis depth variation. The tick marks on the vertical axes are 500 m apart. Dashed line with labels corresponds to 3,000 m depth for the profile. (a) north of the 15°20'N Fracture Zone. (b) south of the 15°20'N Fracture Zone.

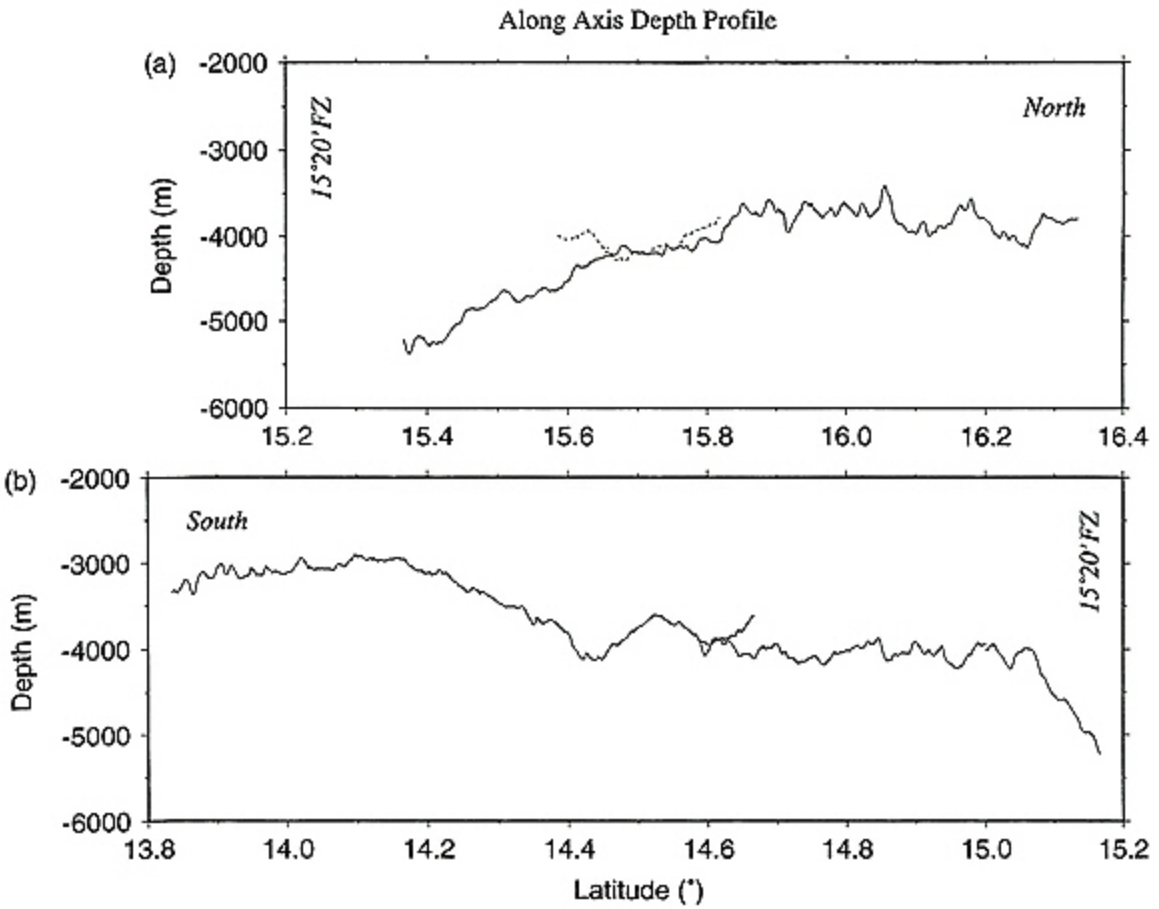

Fig. 9 Along-axis depth variation. (a) north of the 15°20'N Fracture Zone. Dashed line shows overlapping spreading center. (b) south of the 15°20'N Fracture Zone.

lineated rift mountains are dominant in the western flank. South of 14°40'N, the topographic lineation shows only the N-S trending, and the off-axis morphology is symmetrical. The depths of the ridge flanks in this portion are the shallowest in the study area.

Four major segments are recognized along the ridge axis in the study area. North of 15°50'N, axial depth is nearly constant at about 3,800 m (Figure 9(a)). From 15°50'N to the fracture zone, the axial depth increases gradually. Between 14°35'N and 15°05'N, the axial depth is constant at about 4,000 m (Figure 9(b)). These is an isolated deep at 14°25'N. The axial depth decreases toward the south.

3.2 Geomagnetic Anomaly

Lineation patterns of geomagnetic anomalies are unclear in the ridge flanks, even the central anomaly magnetic high in the median valley (Figures 10 and 11). The patterns of geomagnetic total force can be highly skewed because the study area is situated in a low latitude region. Magnetization distribution, calculated from the geomagnetic total force anomalies, can show magnetic lineation patterns related to plate spreading. Crustal magnetization was calculated using the method of Parker and Huestis (1974), which took into account the effect of bathymetry. A uniform magnetic source layer with thickness of 500 m was assumed. The direction of magnetization of the source layer was assumed to be oriented parallel to an geocentric dipole field (Figure 12).

The major isochron was identified preliminarily using the polarity time scale of Cande and Kent (1992). The mean spreading rate is consistent with the full spreading rate of 26.7 km/m.y. calculated from the model of global plate motion (DeMets et al., 1990). The geomagnetic lineation pattern is, however, still unclear and discontinuous after this deskew operation, except the area south of 14°40'N. The observed patchy lineation pattern is consistent with limited basaltic magma supply over a period of several million years, compared with more magmatically robust parts of the Mid-Atlantic Ridge.

The highest geomagnetic anomaly is situated at the western ridge-transform intersection. The result suggests that the most active volcanism is occurring at this region: this is consistent with the submersible observation. South of the fracture zone, magnetization highs are not located along the median valley. The result may suggest an abnormal mode of seafloor spreading in this region. Low amplitude magnetization variation of the ridge flanks in the south of the fracture zone, compared with that in the north of the fracture zone, was observed

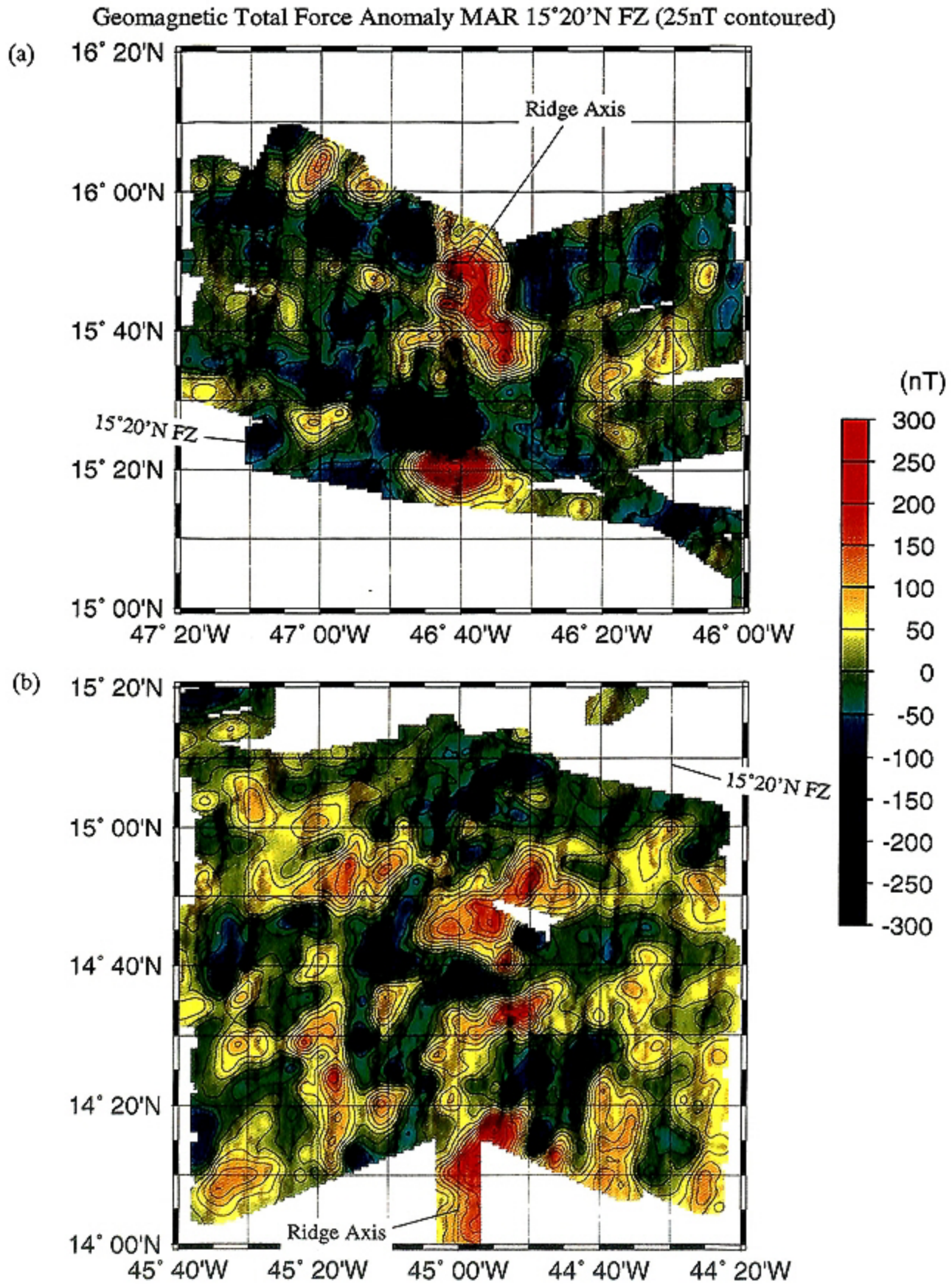

Fig. 10 Geomagnetic total intensity anomaly. Contours are at 25 nT intervals. Heavy black lines show bathymetry with 1,000 m contour intervals. (a) north of the 15°20'N Fracture Zone. (b) south of the 15°20'N Fracture Zone.

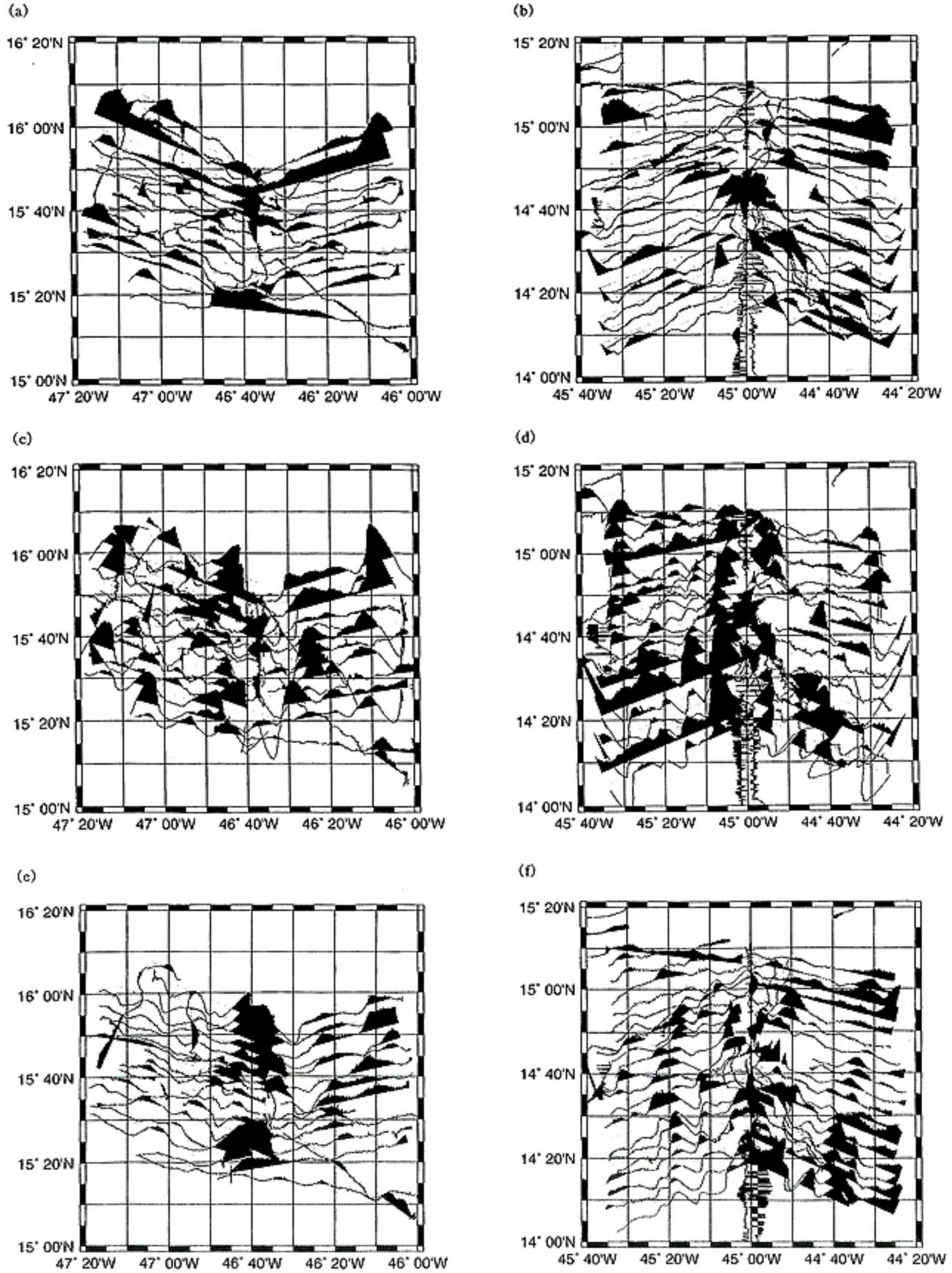

Fig. 11 Vector geomagnetic anomaly along ship tracks.(a)X(northward)component anomaly north of the 15°20'NFracture Zone. (b) X(northward) component anomaly south of the 15°20'N Fracture Zone. (c) Y (eastward) component anomaly north of the 15°20'N Fracture Zone. (d) Y (eastward) component anomaly south of the 15°20'N Fracture Zone. (e) Z (downward) component anomaly north of the 15°20'N Fracture Zone. (f) Z (downward) component anomaly south of the 15°20'N Fracture Zone.

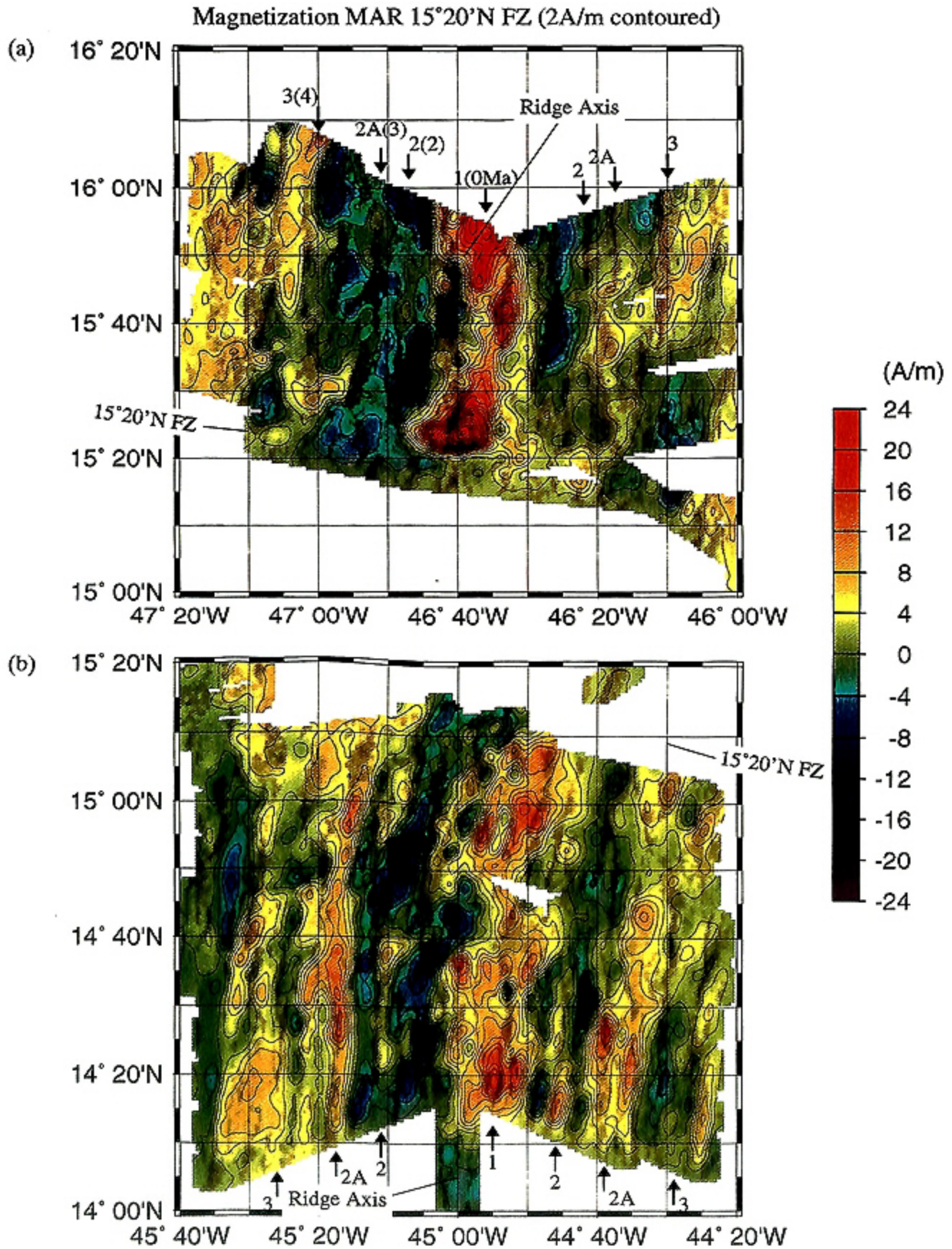

Fig. 12 Magnetization distribution. Contours are at 2 A/m intervals. Heavy black lines show bathymetry with 1,000 m contour intervals. (a) north of the 15°20'N Fracture Zone. (b) south of the 15°20'N Fracture Zone.

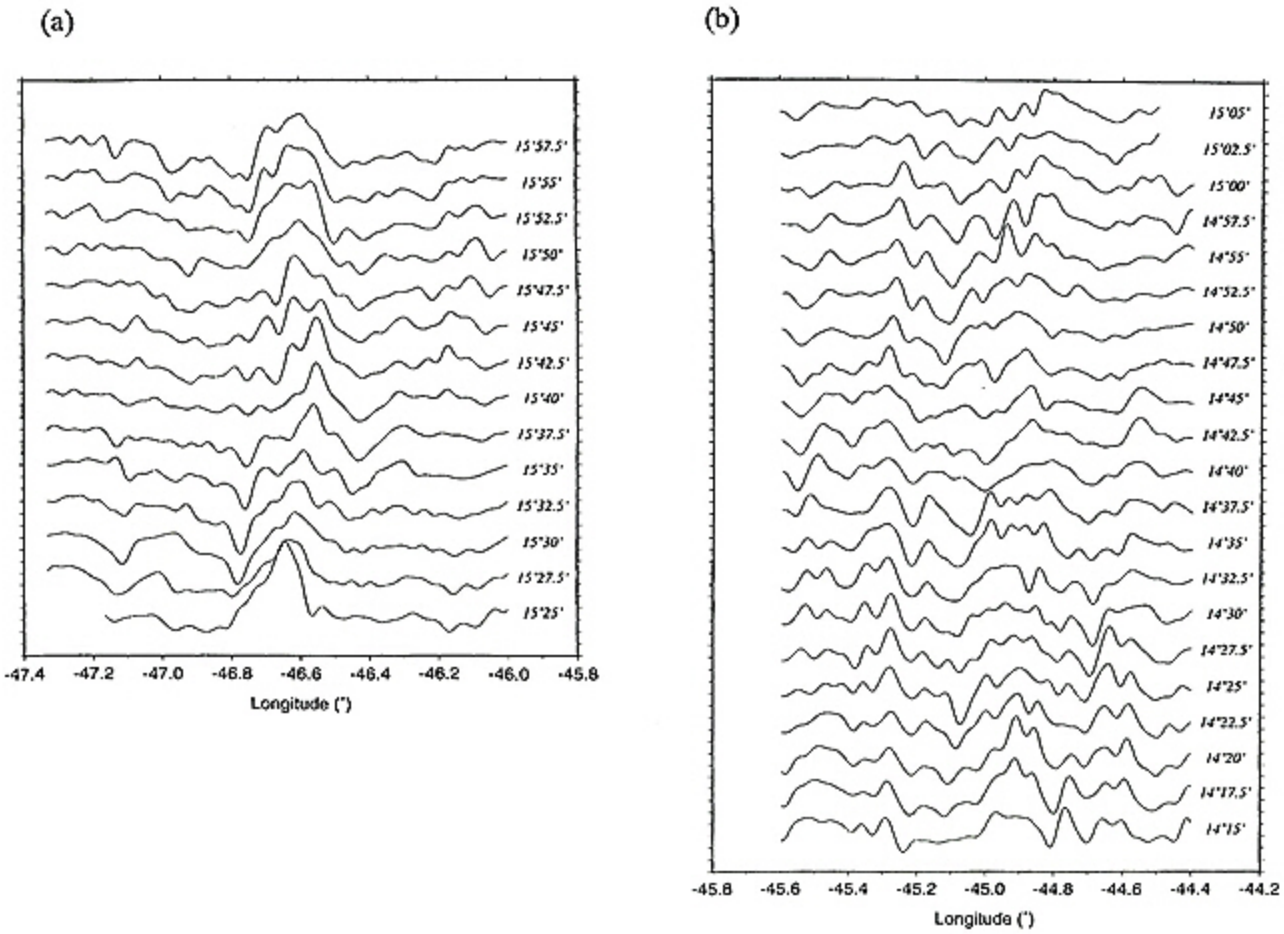

Fig. 13 Across-axis variation of magnetization. The tick marks on the vertical axes are 5 A/m apart. Dashed line with labels corresponds to 0 A/m for the profile. (a) north of the 15°20'N Fracture Zone. (b) south of the 15°20'N Fracture Zone.

(Figures 12 and 13). This result is consistent with magnetic measurements of rocks sampled by the Shinkai 6500 (Joshima et al., 1999). This result suggests weathering of basalt due to tectonic spreading, or else the geochemistry of basalts is different from the north region.

3.3 Gravity Anomaly

Free-air gravity anomalies obtained in this cruise are shown in Figure 14. The free-air gravity anomaly data are merged with the gravity anomaly data derived from satellite altimetry (Sandwell and Smith, 1997) to cover the unsurveyed area. Mantle Bouguer correction was calculated using the method of Kuo and Forsyth (1988). The crust was assumed to have constant thickness of 6 km that follows the seafloor relief. The assumed density of the crustal layer is 2,700 kg/m^3, and that of the underlying mantle is 3,300 kg/m^3. The global predicted bathymetric data (Smith and Sandwell, 1994) were employed to fill the unsurveyed area. Mantle Bouguer anomaly was obtained by subtracting the mantle Bouguer correction from the free-air gravity anomaly.

Low amplitude "bull's eye" mantle Bouguer anomalies, compared with more magmatically robust parts of the Mid-Atlantic Ridge, were observed on the ridge segments flanking the active transform fault (Figures 15 and 16). This is probably due to a limited magma supply that has not generated thick igneous oceanic crust. The gravity data support the conclusion that the magma-starved nature of this region is a long lived phenomenon. Gravity anomaly maps show concentric, semi-circular contours surrounding these gravity lows, becoming less negative toward the fracture zone from the north and the south. The largest gravity anomalies are "bull's eye" lows along the ridge axis at the northernmost and southernmost limits of our survey area, though some of them fail to show their complete shapes due to the limitation of the surveyed area. The center of the largest anomaly is located at 14°00'N and the amplitude amounts to -60 mgals (Figure 15(b)). The simplest interpretation of these data seems to be that the large gravity lows represent the centers of unusually large magmatic segments at approximately 16°N and 14°N, probably as a result of 3-dimensional focusing of melt generation processes in the mantle-dominating tectonics and geodynamics in this region.

Relative high mantle Bouguer anomalies in places (shown by "H"s in Figure 15) reflect that relative high density materials are situated at shallow depth. The density structure or crustal thickness is suggested to vary with time over about 2 m.y., thus the tectonic activity may be cyclic. In the north of the fracture zone, the trough of the "bull's eye" anomaly is located just north of the ridge-transform intersection (Figure 15(a)). The result suggests that basaltic crust in the ridge-transform intersection is locally the thickest. This area is a not normal case compared of this paper and will be the subject of another paper.

Appendix

Correction for the Magnetization of the ship's body

The vector geomagnetic field **F** is derived from the observed magnetic field **Ho** as the following formulation (Isezaki, 1986).

$$\mathbf{F} = \mathbf{R}^{-1}(\mathbf{B}\cdot\mathbf{Ho} - \mathbf{Hp})$$

$\mathbf{R}^{-1}$ is the rotation matrix for conversion from the ship coordinate system to the Earth system, which is function of the ship's heading, roll and pitch. **B** and **Hp** are the matrix and vector concerning induced magnetization and the permanent magnetic field of the ship, respectively. 12 coefficients in the **B** and **Hp** are estimated using data collected during "Figure-8 turn"s.

$$\mathbf{B} = \begin{pmatrix} 1.08163 & 0.04863 & -0.01204 \\ -0.03867 & 1.20069 & -0.01185 \\ 0.02414 & 0.11992 & 0.84863 \end{pmatrix}$$

$$\mathbf{Hp} = \begin{pmatrix} -1872.62 \\ 5567.20 \\ -4698.10 \end{pmatrix}$$

Acknowledgements

The authors would like to acknowledge B. Tucholke, J. Lin, and B. Detrick, who provided us with many stimulating scientific discussions. The authors are indebted to the officers and crew of the R/V Yokosuka for their invaluable help at sea. The on-line logging system (Oshida and Furuta, 1995) was useful for onboard data processing. The GMT software package (Smith and Wessel, 1990; Wessel and Smith, 1991) was used for display purposes.

References

Buchanan, S. K., R. A. Scrutton, R. A. Edwards, and R. B. Whitmarsh, "Marine magnetic data processing in equatorial regions off Ghana", *Geophys. J. Int.*, 125, 123-131 (1996).

Cande, S. C., and D. V. Kent, "A new geomagnetic polarity timescale for the late Cretaceous and Cenozoic", J. Geophys. Res., 97, 13,917-13,951 (1992).

Cannat, M., Y. Lagabrielle, N. de Coutures, H. Bougault, J. F. Casey, L. Dmitriev, and Y. Fouquet, "Ultramafic and gabbroic exposures at the Mid-Atlantic Ridge: Geological mapping in the 15°N region", Tectonophys., 279, 193-214 (1997).

Casey, J. F., M. G. Brass, T. Fujiwara, T. Matsumoto, P. B. Kelemen, and Scientific party, "Megamullions along the Mid-Atlantic Ridge between 14 and 16N: Results of leg 1", JAMSTEC/WHOI MODE 98 survey, (abstract), EOS Trans. AGU, 79(45), 920 (1998).

DeMets, C., R. G. Gordon, D. F. Argus, and S. Stein, "Current plate motions", Geophys. J. Int., 101, 425-478 (1990).

Fujiwara, T., T. Matsumoto, M. Joshima, and A. Takeuchi, "Bathymetry, geomagnetic and gravity anomalies of the Mid-Atlantic Ridge near the 15°20'N Fracture Zone", Abstracts 1999 Japan Earth Planet. Sci. Joint Mtg., D-007 (1999) (in Japanese).

IAGA Division V WG 8, "International Geomagnetic Reference Field, 1995 revision", J. Geomag. Geoelectr., 47, 1,257-1,261 (1995).

Isezaki, N., "A new shipboard three component magnetometer", Geophysics, 51, 1,992-1,998 (1986).

Joshima, M., T. Fujiwara, T. Matsumoto, and A. Takeuchi, "3 component geomagnetic field measurements near the sea-floor of MAR around the Cape Verde Fracture Zone", Abstracts 1999 Japan Earth Planet. Sci. Joint Mtg., D-008 (1999) (in Japanese).

Kelemen, P. B., T. Matsumoto, and Shipboard scientific party, "Geological results of MODE 98, Leg 1: JAMSTEC/WHOI Shinkai 6500 submersible and shipboard geophysics cruise to 15 N, Mid Atlantic Ridge", (abstract), EOS Trans. AGU, 79(45), 43 (1998).

Kuo, B. Y. and D. W. Forsyth, "Gravity anomalies of the ridge-transform system in the South Atlantic between 31 and 34.5°S: Upwelling centers and variations in crustal thickness", Mar. Geophys. Res., 10, 205-232 (1988).

Matsumoto, T., P. B. Kelemen, and Onboard scientific party, "Preliminary result of the precise geological mapping of the Mid-Atlantic Ridge 14-16N - tectonic extension along the magma-poor ridge axis" (abstract), EOS Trans. AGU, 79(45), 46 (1998).

Oshida, A. and T. Furuta, "New geophysical data logging system of R/V Yokosuka", JAMSTEC J. Deep Sea Res., 11, 421-433 (1995).

Parker, R. L. and S. P. Huestis, "The inversion of magnetic anomalies in the presence of topography", J. Geophys. Res., 79, 1,587-1,593 (1974).

Sandwell, D. T. and W. H. F. Smith, "Marine gravity

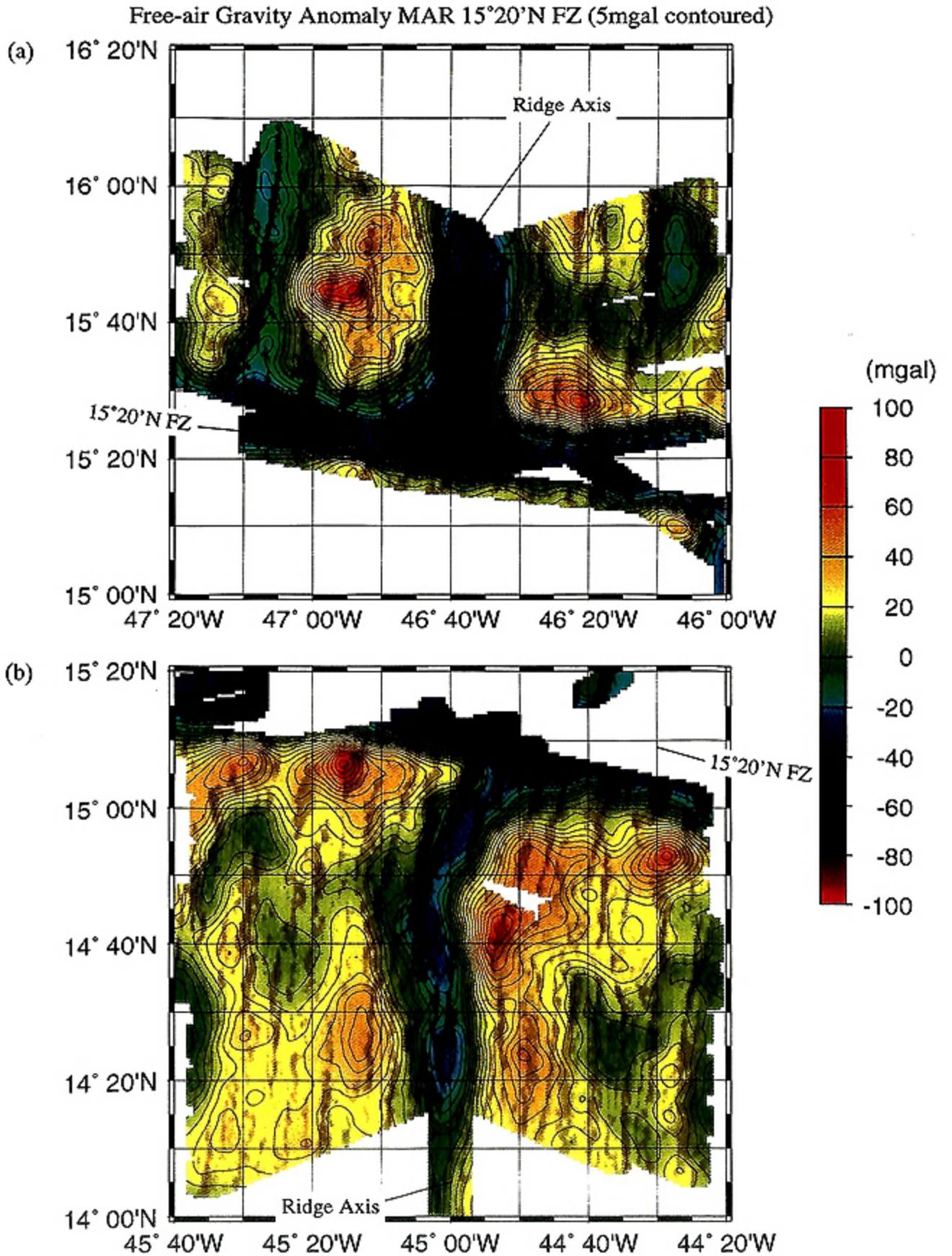

Fig. 14 Free-air gravity anomaly. Contour interval is 5 mgal. Heavy black lines show bathymetry with 1,000 m contour intervals. (a) north of the 15°20'N Fracture Zone. (b) south of the 15°20'N Fracture Zone.

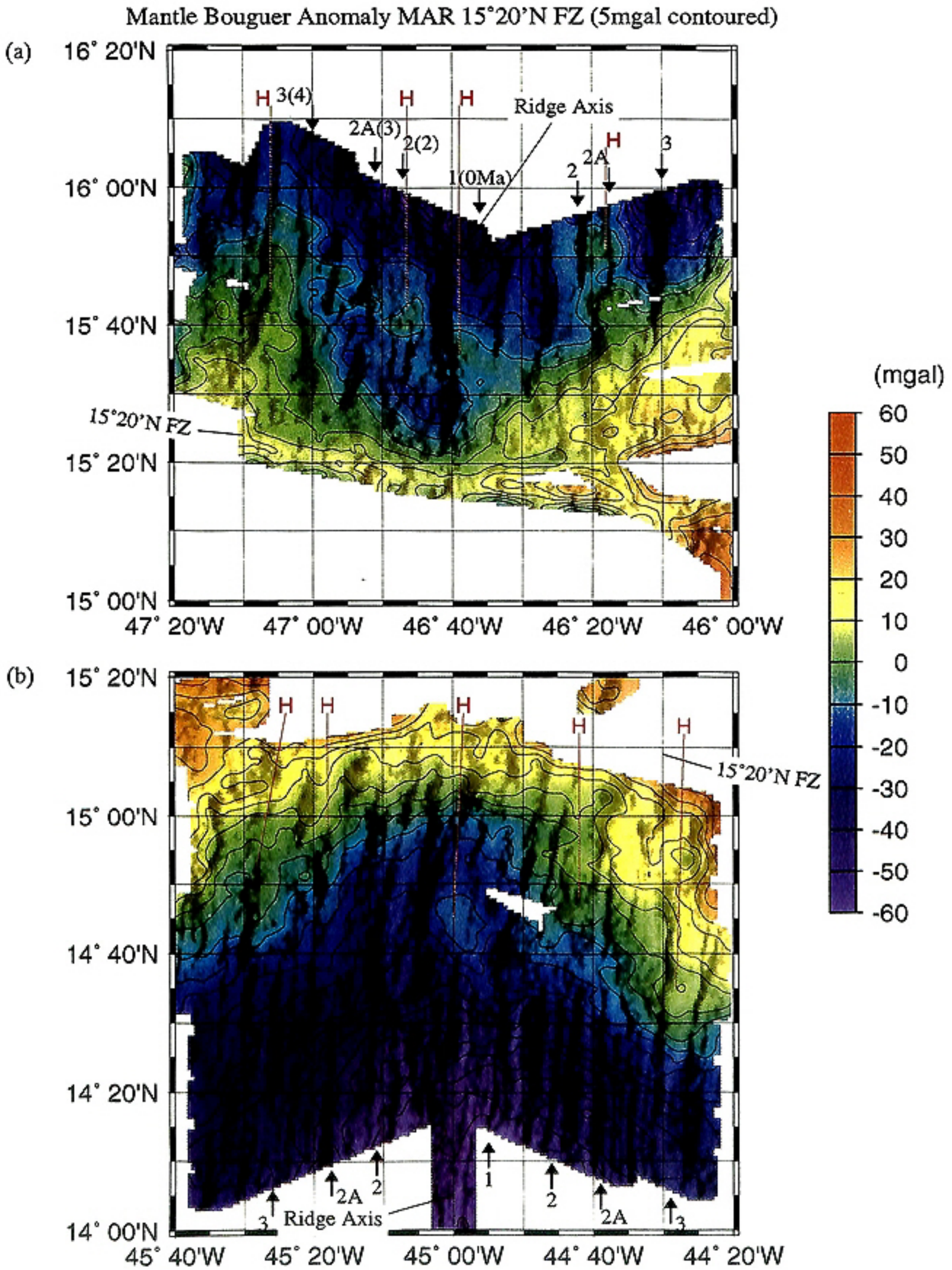

Fig. 15 Mantle Bouguer anomaly. Contour interval is 5 mgal. Heavy black lines show bathymetry with 1,000 m contour intervals. (a) north of the 15°20'N Fracture Zone. (b) south of the 15°20'N Fracture Zone.

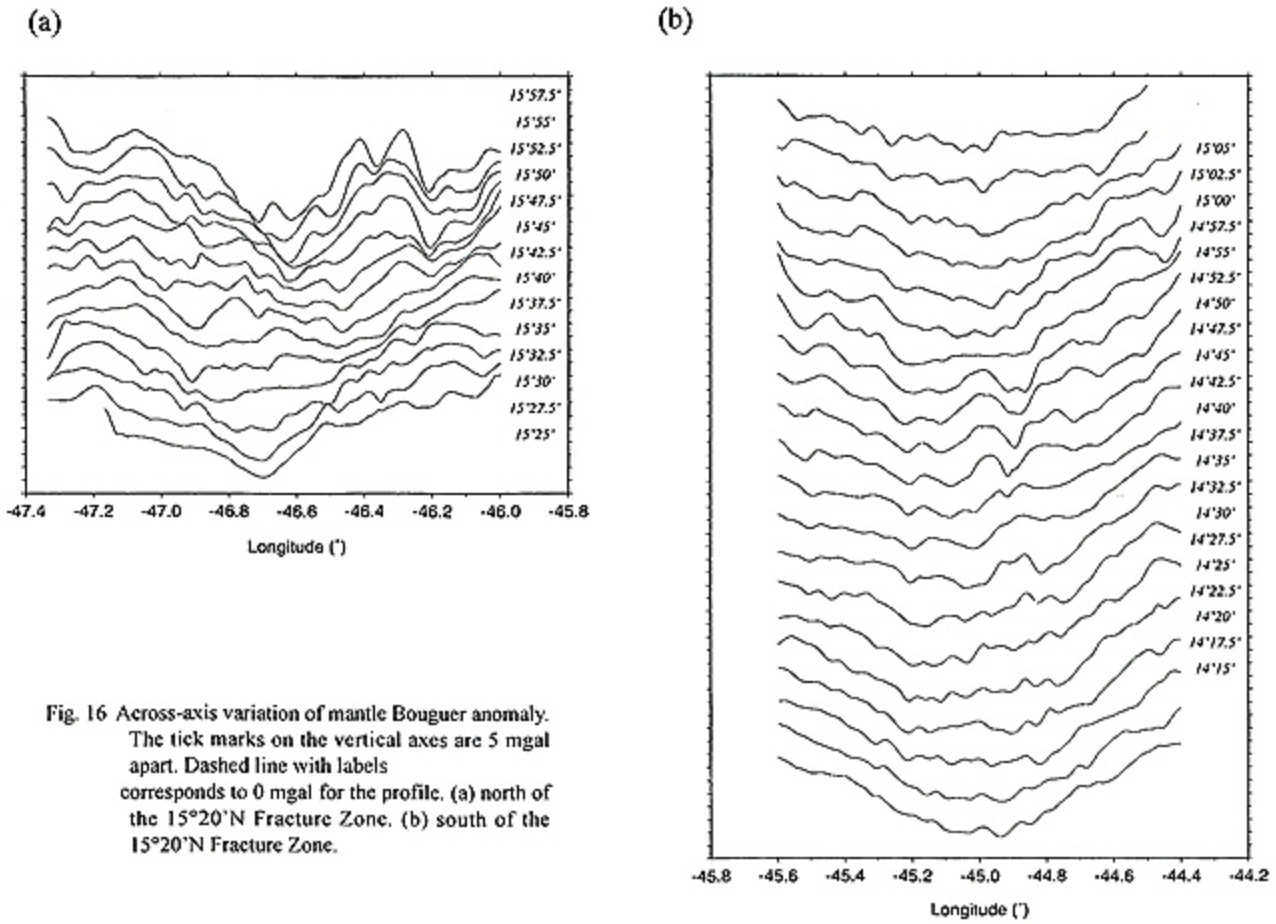

Fig. 16 Across-axis variation of mantle Bouguer anomaly. The tick marks on the vertical axes are 5 mgal apart. Dashed line with labels corresponds to 0 mgal for the profile. (a) north of the 15°20'N Fracture Zone. (b) south of the 15°20'N Fracture Zone.

anomaly from Geosat and ERS 1 satellite altimetry", J. Geophys. Res., 102, 10,039-10,054 (1997).

Smith, W. H. F. and D. T. Sandwell, "Bathymetric prediction from dense altimetry and sparse shipboard bathymetry", J. Geophys. Res., 99, 21,803-21,824 (1994).

Smith, W. H. F. and P. Wessel, "Gridding with continuous curvature splines in tension", Geophysics, 55, 293-305 (1990).

Wessel, P. and W. H. F. Smith, "Free software helps map and display data", EOS Trans. AGU, 72, 441, 445-446 (1991).

(原稿受理：1999年8月17日)